Comparison and Examination of Dynamic Frameworks of IAP and OSU AGCM

Zhang Xuehong (张学洪) and *Liang Xinzhong* (梁信忠)
Institute of Atmospheric Physics, Academia Sinica, Beijing 100011
Received July 11, 1988

ABSTRACT

A brief description of the dynamic framework of the IAP 2-L AGCM (referred as "IAP DF") is presented in contrast with the corresponding "OSU DF" and preliminary comparison and examination of the IAP DF and the OSU DF with the aid of numerical experiments using a set of baroclinic Rossby–Haurwitz wave initial conditions is performed.

The results of the numerical experiments show that both the IAP DF and the OSU DF are long-term computational stable and are able to simulate the fundamental behavior of the Rossby–Haurwitz wave under the limitation of 7.5 minutes time interval. In the respect of the prediction of the large–scale wave, the IAP DF is better than the OSU DF, however, the OSU DF gives better predictions of zonal mean status than the IAP DF does. Another important contrast is that the level of small–scale noise of the IAP DF is higher than the OSU DF, on the contrary, the damping effect of the OSU DF on large–scale vortex field is stronger than the IAP DF.

I. INTRODUCTION

In recent years, the Institute of Atmospheric Physics, Academia Sinica (IAP) developed a two–level Atmospheric General Circulation Model (IAP AGCM, Zeng, Yuan, Zhang, Liang and Bao, 1986). The IAP AGCM consists of two main parts: dynamic framework and physical processes. The so–called "dynamic framework" (DF) refers to the version of the dynamic system of equations used in AGCM and the corresponding finite–difference schemes (not including source and sink terms). The IAP DF is, to a certain extent, independent on other GCMs in the world and has some unique features. For instance, the introduction of "Standard Stratification Approximation" (Zeng, 1979) in the dynamic equations, the design of "Available Energy" conservative finite–difference schemes (Zeng, Yuan, Zhang and Bao, 1985) and some special considerations concerning computational stability and flexibility (Zeng, Ji and Yuan, 1982; Zeng and Zhang, 1981). On the other hand, there have already been several excellent GCMs in the world, in which rather comprehensive diabatic forcing–feedback and dissipation processes are included. One of them is the OSU 2–Level AGCM. Therefore, as the first step of developing IAP GCM, the current IAP AGCM is basically a combination of the IAP DF and the physics of the OSU AGCM and also absorbs some useful methods and techniques of other models (Liang, 1986). Thus, it is necessary to give a comparison between the IAP DF and the OSU DF—that is just the topics of this paper.

In the second section of this paper, a brief description of the IAP DF will be presented in contrast with the OSU DF (Ghan et al, 1982). There are some important differences between the IAP DF and the OSU DF in the respects of the variant of dynamic equations, grid systems, space finite–difference schemes and time integration methods and filtering or smoothing techniques. Some of them mey be direct reasons for producing differences between the two GCM's climatic simulations (Liang, 1986) because that the two GCMs have almost the same physical processes.

The IAP DF and the OSU DF, however, have something in common, in which the same horizontal resolutions and the same vertical layers provide a possibility of comparing the two models under an equal condition by using numerical experiments. One of the difficulties, in doing so, is the choice of the initial conditions of the experiments because that we have to understand the behavior of the solution corresponding to the initial conditions in advance in order to judge which model is better than the other and in which respect or vise versa. In other words, we need such a kind of initial conditions that can be used in estimating not only the "second–kind predictability" but also the "first–kind predictability" (Smagorinsky, 1979). Fortunately, we have found a kind of baroclinic Rossby–Haurwitz waves (including linear and nonlinear waves) and shown the possibility of testing the long–term behavior of GCM's dynamic framework using them (Zhang, Zeng and Bao, 1986; Zhang, Bao, Yuan and Zeng, 1987).

In the third section of this paper, a set of numerical experiments with the Rossby–Haurwitz wave initial conditions will be described and a preliminary comparison between the IAP DF and the OSU DF will be presented. Both the IAP DF and the OSU DF are long–term computational stable and are able to simulate the basic behavior of the Rossby–Haurwitz wave as a propagating wave on sphere. The zonal mean "climate status" predicted by the OSU DF is better than the IAP DF, however, the large–scale vortex fields predicted by the IAP DF are better than the OSU DF although the vortex fields are weakened, to different extent, in both predictions. It seems that too strong damping is included in the OSU DF which makes large–scale vortex underestimated. On the contrary, the level of the noise in the IAP DF should be controlled further. Actually, Shapiro filtering technique has been successfully used in the climate simulation experiments of the IAP AGCM (Liang, 1986).

II. A BRIEF DESCRIPTION OF IAP DF

1. *Dynamic System of Equations*

Both the IAP DF and the OSU DF use the baroclinic primitive equations in σ–coordinates on sphere, where

$$\sigma \equiv \frac{p - p_T}{\pi}, \qquad \pi \equiv p_s - p_T \tag{1}$$

(Ghan et al, 1982). Considering the benefit of approximate calculations, however, the IAP DF uses another version of the equations, of which the main characteristics are as follows.

(1) A static "standard atmosphere" described by $\tilde{T}(p)$, $\tilde{\varphi}(p)$ and $\tilde{p}_s(\theta,\lambda)$ is introduced into the basic equations and the corresponding perturbed variables

$$T' \equiv T - \tilde{T}(p), \tag{2}$$

$$\varphi' \equiv \varphi - \tilde{\varphi}(p), \tag{3}$$

and

$$p_s' \equiv p_s - \tilde{p}_s(\theta,\lambda) \tag{4}$$

are taken as the state parameters of the model atmosphere. Meanwhile, the adiabatic heating term of the thermodynamic equation is linearized as

$$\frac{RT}{p}\omega \approx \frac{R\tilde{T}}{p}\omega \ , \tag{5}$$

that is the so-called "Standard Stratification Approximation" (Zeng, 1979). Table 1 and Table 2 give the comparison between the model's standard atmosphere and the observational standard atmosphere (U.S. Standard Atmosphere, 1976). It can be seen that the model's standard atmosphere can approximate the observational one with rather high accuracy. Thus, the introduction of $\tilde{T}(p)$, $\tilde{\varphi}(p)$ and $\tilde{p}_s(\theta,\lambda)$ is favorable for deducting the truncation error of pressure gradient terms near mountain slopes.

Table 1. Temperatures of the Model's and Observed Standard Atmospheres

p (hPa)	200	300	400	500	600	700	800	900	1013
$\tilde{T}(p)$ (K)	216	231	243	253	261	269	275	282	288
U.S. Standard Atmosphere, 1976	216.6	228.7	241.4	252.1	260.8	268.3	275.4	281.7	288

Table 2. Heights of the Model's and Observed Standard Atmospheres

p (hPa)	200	300	400	500	600	700	800	900	1013
$\frac{1}{g}\tilde{\varphi}(p)$ (m)	11840	9186	7191	5574	4203	3008	1946	986	0
U.S. Standard Atmosphere,1976	11800	9200	7200	5600	4200	3000	1950	1000	0

(2) The practical prognostic variables of the momentum equations and the thermodynamic equation of the IAP DF are

$$U \equiv Pu, \qquad V \equiv Pv \tag{6}$$

and

$$T \equiv \frac{R}{c_0} PT' \tag{7}$$

where

$$P \equiv \sqrt{\pi} \tag{8}$$

and the prognostic variables of the OSU DF are

$$U \equiv \pi u, \qquad V \equiv \pi v \tag{9}$$

and

$$T = \tilde{T}(p) + T' \tag{10}$$

Correspondingly, the nonlinear terms of the momentum and the thermodynamic equations are written as

$$\frac{1}{a\sin\theta}\left(\frac{\partial uF}{\partial\lambda}+\frac{\partial v\sin\theta F}{\partial\theta}\right)+\frac{\partial\dot{\sigma}F}{\partial\sigma}-\frac{F}{2}\left[\frac{1}{a\sin\theta}\left(\frac{\partial u}{\partial\lambda}+\frac{\partial v\sin\theta}{\partial\theta}\right)+\frac{\partial\dot{\sigma}}{\partial\sigma}\right], \qquad (F=U,V,T)$$

and

$$\frac{1}{a\sin\theta}\frac{\partial uF}{\partial\lambda}+\frac{1}{a}\frac{\partial vF}{\partial\theta}+\frac{\partial\dot{\sigma}F}{\partial\sigma}, \qquad (F=U,V,T)$$

for the IAP DF and the OSU DF respectively. The latter is the pure flux form and the fromer is practically the combination of flux form and advection form.

(3) Defining

$$e_k \equiv \frac{1}{2}(U^2 + V^2), \tag{11}$$

$$e_a \equiv \frac{1}{2}T^2 \tag{12}$$

and

$$e_{as} \equiv \frac{R\tilde{T}(\tilde{p}_s)}{\tilde{p}_s}\frac{1}{2}(p_s')^2 \tag{13}$$

as kinetic energy, "available potential energy" and "available surface potential energy", we shall have, under the "Standard Stratification Approximation",

$$\frac{\partial}{\partial t}\int_0^{2\pi}\int_0^{\pi}\int_0^{1}[e_k + e_a + e_{as}]d\sigma \cdot a^2\sin\theta d\theta d\lambda = 0, \tag{14}$$

i.e. the total "available energy" conservation for the IAP DF. It means that it is possible to use the IAP DF to design finite-difference schemes which can conserve the total available energy rather than the total energy. Also, it is possible to design "perfect" available energy conservative time-space finite-difference schemes because of the use of the special form of prognostic variables (Zeng and Zhang, 1981).

2. *Grid System and Finite-Difference Schemes*

(1) *Grid system*

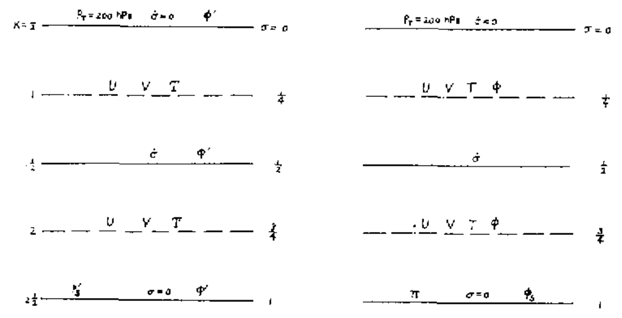

Fig.1 Vertical Structures of IAP DF (left) and OSU DF (right)

The horizontal grid systems of the IAP DF and the OSU DF are the so-called "C-grid" and the "B-grid" (Arakawa, 1977) respectively. From the viewpoint of describing the dispersion of inertia-gravity waves, B-grid is better than C-grid, however, from the viewpoint of computational economy, C-grid is better than B-grid. In order to make a further comparison, we have already designed a dynamic framework based on B-grid (Zeng and Zhang, 1987).

Fig.1 shows the vertical structures of the IAP DF and the OSU DF, in which the only difference between the two models is that the geopotential is placed at the interfaces between two layers in the IAP DF and at the middle level of the layers in the OSU DF.

(2) *Space finite-difference schemes*

The importance of conserving certain integral properties of continuous problem, e.g. conservation of mass, energy etc., has been emphasized in the design of the finite-difference schemes of the IAP DF (Zeng et al, 1982). In the current IAP DF, we put a particular attention in describing the conversions between kinetic energy, available potential energy and available surface potential energy in the case of discrete variables. Based on this principle, the total "available energy" conservative space finite–difference schemes are designed for both C–grid and B–grid (Zeng and Zhang, 1987). The total "available energy" conservation is the more effective constraint than common total energy conservation for the gross property of finite–difference schemes because that only the available potential energy and the available surface potential energy are the convertible portions of total potential energy and have same order of magnitude as kinetic energy. From the viewpoint of numerical analysis, the "available energy" conservative scheme is the "quadratic conservative" scheme which is favorable for computational stability.

One of the main features of the space finite–difference of the OSU DF is the use of "enstrophy conservative" scheme of the nonlinear terms of momentum equations (Arakawa, 1977), which is based on the principle of the mean scale conservation in nondivergent flow.

(3) *Time integration and filtering*

It should be pointed out that the conservation of "available energy" is strictly correct only when certain fully–implicit time integration methods being used and in that case a kind of perfect "available energy" conservative space–time finite–difference schemes will be obtained (Zeng and Zhang, 1981). At the present, however, the most simple explicit leap–frog scheme with Shuman's time–average technique of pressure gradient terms is used in the time integration of the IAP DF. Meanwhile, in the polar regions, the Fourier filtering respect to all the time derivatives is performed to avoid the computational instability associated with the convergence of the meridians as the poles are approached.

The time integration method of the OSU DF is a combination of Matsuno scheme, Matsuno–TASU scheme and leap–frog scheme with a longitudinal smoothing of the zonal pressure gradient terms and the zonal mass flux in the polar regions.

3 *A Comparison of IAP DF and OSU DF*

In order to gain a practical understanding of the difference between the IAP DF and the OSU DF, we performed two parallel numerical experiments, in which both the IAP DF and the OSU DF were integrated up to 100 model's days with the same initial conditions given by a baroclinic linear Rossby–Haurwitz wave. On this basis, preliminary comparison and examination of the two models have been completed. The initial conditions, computational stabilities and some representative results of the two integrations will be described.

(1) *Initial conditions*

The formulae of the baroclinic linear Rossby–Haurwitz waves are as follows:

$$u_k = a\bar{\Omega}_k \sin\theta + aA_k \sin^{m-1}\theta[(m+1)\cos^2\theta - 1]\cos m\lambda, \tag{15}$$

$$U_k = maA_k \sin^{m-1}\theta\cos\theta\sin m\lambda, \tag{16}$$

$$T_k = T_0(\theta;\bar{\Omega}_{k\pm\frac{1}{2}}, A_{k\pm\frac{1}{2}}) + T_1(\theta;\bar{\Omega}_{k\pm\frac{1}{2}}, A_{k\pm\frac{1}{2}})\cos m\lambda$$
$$+ T_2(\theta;\bar{\Omega}_{k\pm\frac{1}{2}}, A_{k\pm\frac{1}{2}})\cos 2m\lambda, \tag{17}$$

$$P_s = P_0(\theta;\bar{\Omega}_{K+\frac{1}{2}}, A_{K+\frac{1}{2}}) + P_1(\theta;\bar{\Omega}_{K+\frac{1}{2}}, A_{K+\frac{1}{2}})\cos m\lambda + P_2(\theta;\bar{\Omega}_{K+\frac{1}{2}}, A_{K+\frac{1}{2}})\cos 2m\lambda. \tag{18}$$

where

$$\begin{cases} \bar{\Omega}_k = \frac{1}{2}(\bar{\Omega}_{k-\frac{1}{2}} + \bar{\Omega}_{k-\frac{1}{2}}), \\ A_k = \frac{1}{2}(A_{k-\frac{1}{2}} + A_{k-\frac{1}{2}}), \end{cases} \tag{19}$$

and T_0, T_1, T_2; P_0, P_1, P_2 can be derived from Phillips's formula (Phillips, 1959). The values of the parameters are set as:

$$\begin{cases} m = 4, \\ \bar{\Omega}_{k-\frac{1}{2}} = (0.25, 0.20, 0.15) \times 10^{-6}\mathrm{s}^{-1}, \\ A_{k-\frac{1}{2}} = 0.15 \times 10^{-6}\mathrm{s}^{-1}. \qquad (k = 1,2,3) \end{cases} \tag{20}$$

Differing from the traditional Rossby–Haurwitz wave (Phillips, 1959), the above initial conditions may determine a better approximate propagating wave solution to the primitive equations (Zhang et al, 1986). In our case, the solution should be a westward propagating wave with the phase–speed of −14 longitudinal degrees per day.

Fig.2 shows the initial surface pressure of the Rossby–Haurwitz wave, which is independent on the models. The initial 500 hPa heights of the IAP DF and OSU DF are slightly different that comes from the different algorithms of static equations.

(2) *Computational stability*

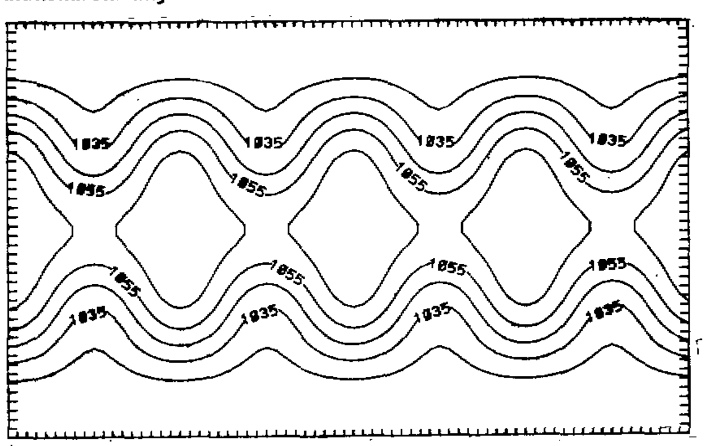

Fig.2. Surface pressre of 2–L RH4 on 0 th day (in hPa).

With the initial conditions mentioned above, both the IAP DF and the OSU DF are computational stable under the limitation of 7.5 minutes time step. Fig.3 gives the surface pressure fields of the 100th day predicted by the two models respectively.

Usually, the time step of the IAP DF is 7.5 minutes and the time step of the OSU DF is 10 minutes. However, our current numerical experiments seem to show that 10 minutes time step is too large to keep the computational stability of the OSU models. Actually, a running of the OSU DF, with the same initial conditions but 10 minutes time step, collapsed at the 5th model's day.

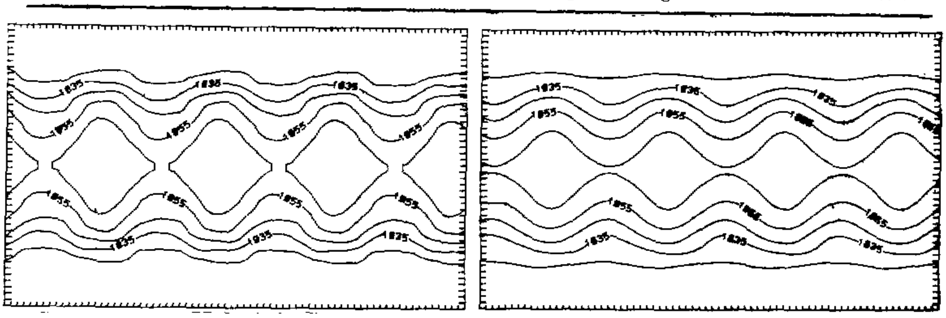

Fig.3(a). Surface pressre of 2–L RH4 on 100th day (IAP DF). (b) Surface pressre of 2–L RH4 on 100th day (OSU DF).

(3) *Kinetic energy and available energy*

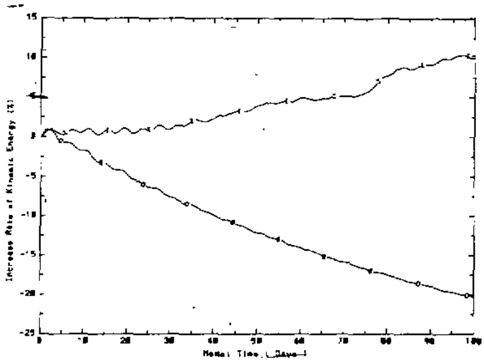

Fig.4. Temporal variation of kinetic energy (I–IAP DF, O–OSU DF).

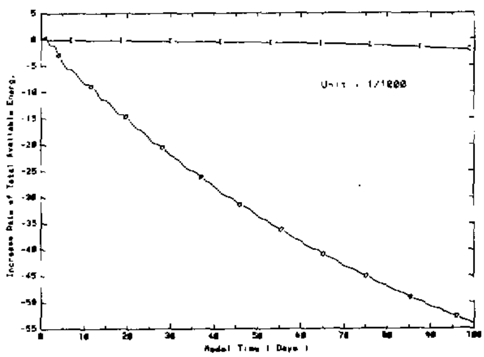

Fig.5. Temporal variation of available energy (I–IAP DF, O–OSU DF).

Fig.4–5 show the temporal variations of the kinetic energy and the total "available energy" of the two integrations. As it is expected, the IAP DF does conserve it's total "available energy" with rather high accuracy. At the 100th day, the variation rate of the total "available energy" of the IAP DF is only −0.2% of it's initial value, however, the total "available energy" of the OSU DF decrease by 5% at the same time.

Another sharp contrast is the variation of kinetic energy of the two models: by the 100th day the kinetic energy of the IAP DF has increased by 10% and the kinetic energy of the OSU DF has decreased by 20% .

(4) *Zonal mean pressure, wind and temperature*

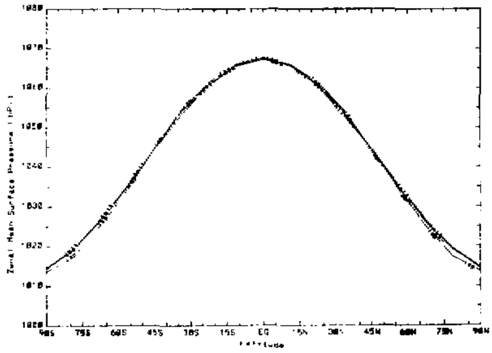

Fig.6. Zonal mean surface pressure averaged over 100 days (Init–initial).

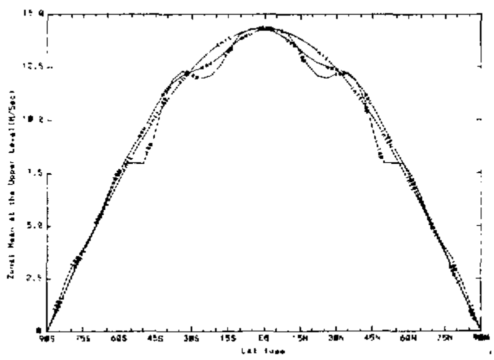

Fig.7. Zonal mean upper level wind averaged over 100 days (Init–initial).

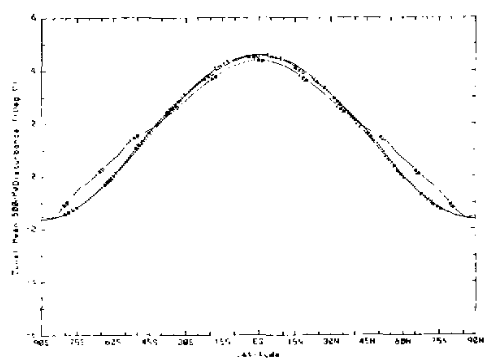

Fig.8. Zonal mean 500 hPa disturbance temperature averaged over 100 days.

Figs.6–8 are respectively the zonal mean pressure, wind and temperature averaged over the 100 days for the two model's integrations and the corresponding initial distributions.

Generally speaking, both the IAP DF and the OSU DF are able to keep these zonal mean status with little changes during such a long–term integration. However, the errors of the zonal mean status simulated by the IAP DF are greater than the results of the OSU DF. For instance, there are two peaks of the error of upper level wind of the IAP DF at 25 deg. and 50 deg. latitude respectively and the maximum error is 1.5 m / s, and only one peak appeared in the results of the OSU DF with the maximum error of 0.6 m / s.

The more interesting point is that the zonal mean distribution of 500 hPa disturbance temperature that is one of important characteristics of the baroclinity of the Rossby–Haurwitz wave is basically maintained during the long–term integrations of both two models. Again, the zonal mean 500 hPa temperature simulated by the OSU DF is better than by the IAP DF.

Additionally, combining Fig.4 and Fig.7, we can see that the decreasing of total kinetic energy in the OSU DF is mainly caused by the decreasing of the vortex kinetic energy because of the conservation of zonal kinetic energy.

(5) *Amplitude and phase of the wave*

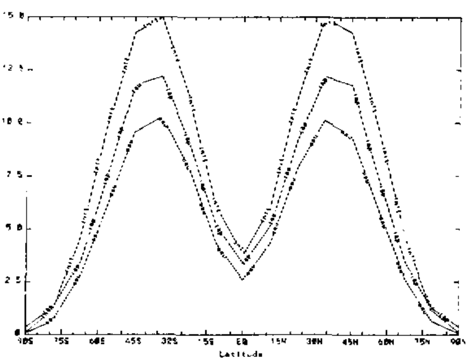

Fig.9. Latitudinal profile of the wave No.4 of surface pressure averaged over 100 days in hPa (Init–th initial).

Fig.9 shows the latitudinal distributions of the amplitudes of the wave No.4 averaged over the 100 days for the surface pressure fields of the IAP DF and the OSU DF respectively as well as the initial status. Comparing with the initial status, both the IAP DF and the OSU DF underestimate the amplitude of the wave: the maximum departures from the initial status are 3.1 hPa for the IAP DF and 5.3 hPa for the OSU DF respectively. Considering of the long–term averaging being used, the difference between the two models should be significant. Actually, the more obvious differences can be seen from the 100 day's predictions of the surface pressure given by the two models respectively (see Fig.3). It seems that there are some damping effects on the vortex field in both two dynamic frameworks, but the damping effect in the OSU DF is stronger than the IAP DF.

Table 3 gives the phases of the wave No.4 at the equator on every ten days for the two integrations. The phase–speeds averaged over the 100 days are −13.7 deg. longitude per day for the IAP DF and −13.8 deg. longitude per day for the OSU DF. They are all good approximations to the theoretical phase–speed of the Rossby–Haurwitz wave.

Table 3. Wave Phase Predicted by IAP DF and OSU DF (in degrees longitude)

t (days)	0	10	20	30	40	50	60	70	80	90	100
IAP DF	0	−134	−272	−406	−544	−680	−815	−949	−1087	−1226	−1366
OSU DF	0	−140	−279	−417	−555	−693	−832	−969	−1107	−1246	−1384

This paper was completed in the laboratory for Planetary Atmospheres of SUNY at Stony Brook. We would like to thank Dr. Robert D. Cess for suggesting the project and providing conditions necessary for performing numerical experiments. This work was partially supported by the CO_2 Research Division, Office of Basic Energy Sciences U.S. Department of Energy, under Grant DEFG0285ER60314 to SUNY Stony Brook.

REFERENCES

Arakawa, A. and V. R. Lamb (1977), Computational Design of the Basic Dynamical Processes of the UCLA General Circulation Model, *Methods in Computational Physics*, **17**: 173–265.

Ghan, S. J., J. W. Lingaas, M. E. Schlesinger, R. D. Mobley and W.L.Gates (1982), A Documentation of the OSU Two–Level Atmospheric General Circulation Model, Rep.61, Climatic Research Institute, Oregon State University, Corvallis, OR, 391pp.

Liang, X. Z. (1986), The Design of IAP GCM and the Simulation of Climate and Its Interseasonal Variability, Ph. D. Thesis, 250pp.

Smagorinsky, J. (1979), Overview of the climate modelling problems, GARP Publication Series, No.22 (1979), 1–12.

Zeng, Q. C. (1979), *Physical–Mathematical Basis of Numerical Weather Prediction*, vol.1 Science Press, Beijing, 1979 (in Chinese).

Zeng, Q. C., Z. Z. Ji and C. G. Yuan (1982), Design of Difference Schemes for the Primitive Equations, *Scientia Sinica* (Series B), **25**: No.2, 183–199.

Zeng, Q. C. and X. H. Zhang (1981), Perfect Energy–Conservative Time–Space Finite–Difference Schemes and the Consistent Split Method to Solve the Dynamic Equations of Compressible Fluid, *Scientia Sinica*, 1981, No.11, 1355–1366.

Zeng, Q. C., C. G. Yuan, X. H. Zhang and N. Bao (1985), Tests of the Finite–Difference Schemes of a General Circulation Model, *Acta Meteorologica Sinica*, **43**: 441–449.

Zeng, Q. C., and X. H. Zhang (1987), Available Energy Conservative Finite–Difference Schemes for the Baroclinic Primitive Equations on Sphere, *Chinese Journal of Atmospheric Sciences*, **11**: No.2, 121–142.

Zeng, Q. C., C. G. Yuan, X. H. Zhang, X. Z. Liang and N. Bao (1986), A Global Gridpoint General Circulation Model, In: Short– and Medium–Range Numerical Weather Prediction Collection of Papers Presented at the WMO / IUGG Symposium, Tokyo, Aug. 4–8, 421–430.

Zhang, X. H., Q. C. Zeng and N. Bao (1986), Nonlinear Baroclinic Haurwitz Waves, *Advances in Atmospheric Sciences*, **3**: 330–340.

Zhang X. H., N. Bao, C. G. Yuan and Q. C. Zeng (1987), Studies on the Sensitivity of Dynamical Frame of a General Circulation Model to Initial Conditions, *Scientia Sinica* (Series B), **30**: No.7, 739–750.